KADUNA JOURNAL OF GEOGRAPHY
2026, VOL. 8, No. 1, 675-688
https://doi.org/10.47514/kjg.2026.08.01.065

Research Article

Geospatial Analysis of Hydro-Socioeconomic Factors Driving Flood Risk in the Hadejia River Basin, Nigeria

Muhammad Tukur Murtala [a], Mohammad Hadi Ahmad [b], Abdullahi Balarabe [c], Muktar Ahmad [d], Usman Ado Kibon [c], Edwin Osare Iguisi [c], Auwal Aliyu [b], Nasir Kabiru Muhammad [b]

[a] Centre for Disaster Risk Management and Development Studies, Ahmadu Bello University Zaria, Nigeria.. [b] Zonal Advanced Space Technology Applications Laboratory, Bayero University Kano, National Space Research and Development Agency, Nigeria. [c] Department of Geography and Environmental Management, Ahmadu Bello University, Zaria, Nigeria. [c] Department of Urban Regional Planning, Ahmadu Bello University, Zaria, Nigeria.

ABSTRACT

Flooding is the most recurrent natural hazard in northern Nigeria's Sudano-Sahelian zone. Yet, the combined influence of climatic, hydrological, and socioeconomic drivers of flood risk in the Hadejia River Basin remains poorly quantified. This study identified and spatially analysed the key natural and anthropogenic factors driving flood risk in the basin. Primary data (a three-phase field reconnaissance survey with GPS ground-truthing, August 2023–January 2024) were integrated with secondary datasets: Sentinel-2A imagery, ALOS PALSAR DEM, CHIRPS rainfall (1981–2022), WorldClim temperature, and soil, geological, and socioeconomic layers. Analyses combined supervised maximum-likelihood classification of land use/land cover (LULC), Mann-Kendall trend testing, and GIS-based Multi-Criteria Decision Analysis using the Analytic Hierarchy Process to weight sixteen flood-causative factors grouped into meteorological, hydrological, and socioeconomic criteria. Results show a significant upward trend in annual rainfall ($\tau = 0.377$, $p = 0.0005$) and temperature ($\tau = 0.259$, $p = 0.019$), with the wettest year on record (777.59 mm) in 2022. Between 2013 and 2023, water bodies and dense vegetation contracted by 10 km^2 and 6 km^2, respectively, while farmland and built-up areas expanded by 94 km^2 and 8 km^2, respectively, reducing natural retention and increasing surface runoff. Recorded flood occurrences peaked at 538 events in 2022. Proximity to the river, low elevation, gentle slope, high drainage density, and sparse vegetation emerged as the dominant spatial controls of risk. The study recommends integrating these geospatial outputs into floodplain zoning, early-warning systems, and climate-smart land management to strengthen basin-wide flood resilience.

ARTICLE HISTORY
Submitted 30 July 2026
Accepted 16 September 2026
Published 25 September 2026

GUEST EDITOR
A. M. Ahmed

KEYWORDS
Flood risk; Analytic Hierarchy Process; Land use/land cover change; Mann–Kendall trend; Hadejia River Basin; Nigeria

1 Introduction

Floods are the most frequent and damaging of all weather-related hazards worldwide, accounting for the largest share of people affected by natural disasters and for annual economic losses that average tens of billions of US dollars (Hirabayashi et al., 2013; Kundzewicz et al., 2018). Global analyses consistently project that, under climate change, the frequency and magnitude of riverine and pluvial flooding will intensify, with the largest relative increases in exposure concentrated in Africa and Asia, where population growth, rapid land-use transformation and limited adaptive infrastructure converge (Hirabayashi et al., 2013; IPCC, 2023). Understanding the mechanisms that govern the temporal behaviour of floods – including precipitation, river discharge and flood losses – is therefore a central concern of hydrological science, even though detecting consistent trends in precipitation and discharge remains more difficult than detecting trends in temperature (Kundzewicz et al., 2018).

In West Africa, and particularly in the Sudano-Sahelian belt, flood risk is embedded in a climate regime characterised by strong inter-annual and inter-decadal rainfall variability. The region experienced a prolonged decline in annual rainfall of roughly 20–40% between the 1950s and the 1980s, followed by a partial recovery accompanied by higher rainfall intensity and more frequent extreme events (Nicholson, 2013; Biasutti, 2019). These fluctuations have profoundly altered regional hydrology: the surface area of Lake Chad has contracted dramatically, groundwater levels have migrated, and the discharge regimes of the Chari, Logone, Komadugu Yobe, and Hadejia river systems have been modified (Buma et al., 2016; Chukwuma et al., 2021). At the same time, an expanding body of African case studies demonstrates that flood susceptibility is shaped not only by climatic forcing but by the interaction of climatic, hydrological and anthropogenic drivers, which can be operationalised through GIS-based Multi-Criteria Decision Analysis (MCDA), most commonly the Analytic Hierarchy Process (AHP) (Danumah et al., 2016; Erena & Worku, 2018; Radwan et al., 2019; Aichi et al., 2024; Mokhtari et al., 2024).

Nigeria exemplifies this convergence of hazard and vulnerability. Flooding is now the country's most widespread natural disaster, affecting millions of people and causing repeated large-scale displacement, as

Corresponding Author: Ahmed, M. H. telnettoahmad@gmail.com National Space Research and Development Agency, Abuja, Nigeria.

evidenced by the devastating nationwide floods of 2012 and 2022 (Umar & Gray, 2023; Ologunorisa et al., 2022). The challenge is compounded by the anthropogenic management of hydrological infrastructure, uncoordinated urban expansion into floodplains, and the degradation of wetlands that historically buffered flood peaks (Aderogba, 2012; Eli & Bariweni, 2020; Umar & Gray, 2023). National-scale reviews consistently call for geospatially explicit, locally calibrated flood risk assessments to guide land-use planning and early-warning investment (Umar & Gray, 2023; Tudunwada & Abbas, 2022).

Within Nigeria, the Hadejia River Basin in the Sudano-Sahelian zone of Jigawa State is considered one of the country's most flood-vulnerable basins (Kura et al., 2023). The basin's flood regime reflects a distinctive combination of drivers: a highly variable semi-arid climate; a low-relief floodplain traversed by the Hadejia River and regulated by the upstream Tiga and Challawa Gorge dams; the ecologically sensitive Hadejia Valley Wetland; and rapid agricultural and settlement expansion along the river corridor (Shanono et al., 2023; Shuaibu et al., 2022; Kura et al., 2023). Several studies have examined individual dimensions of this system – hydro-geomorphic flood risk mapping (Shuaibu et al., 2022), flood vulnerability assessment (Kura et al., 2023; Tudunwada & Abbas, 2022), flood frequency analysis (Ibrahim et al., 2016), reservoir operation effects (Shanono et al., 2023), and hydro-climatic influences on flash floods (Nasidi et al., 2023). More recently, Abubakar et al. (2025) applied GIS and AHP to map flood risk and vulnerability in the basin, confirming the continued policy salience of the problem. However, existing work has largely treated climatic variability, land-use/land-cover (LULC) change and socioeconomic exposure in isolation; few studies have integrated long-term climatic trend analysis, multi-criteria geospatial modelling and field-validated evidence within a single framework, and none has systematically combined the sixteen meteorological, hydrological and socioeconomic causative factors considered here for the river corridor communities of the basin.

This fragmented evidence base constitutes the research gap addressed by the present study. Specifically, there is limited understanding of (i) how observed trends in rainfall and temperature over the last four decades relate to the rising frequency of recorded flood events in the basin; (ii) how LULC change between 2013 and 2023 has modified runoff generation and natural retention; and (iii) how the joint spatial configuration of meteorological, hydrological and socioeconomic factors concentrates risk in particular communities along the river. Accordingly, the aim of this study is to identify, quantify and spatially characterise the natural and anthropogenic factors driving flood risk in the Hadejia River Basin. To achieve this aim, the study (1) analyses trends in rainfall and temperature (1981–2022) and in recorded flood occurrences (1984–2023); (2) quantifies LULC dynamics between 2013 and 2023 from satellite imagery; and (3) develops a GIS-based MCDA/AHP framework integrating sixteen flood causative factors to support flood risk mapping and management. The study contributes an empirically grounded, spatially explicit evidence base to support flood risk management by the Hadejia-Jama'are River Basin Development Authority (HJRBDA), state emergency agencies, and local planning authorities, and advances the regional literature by demonstrating how hydro-climatic and socioeconomic drivers can be integrated for one of Nigeria's most vulnerable basins.

2 Materials and Methods

2.1 Study Area

The study focuses on the corridor of the Hadejia River, situated in the Sudano-Sahelian zone of northern Nigeria between latitudes 12°00' and 12°55' N and longitudes 8°59' and 10°40' E (Figure 1). Located in eastern Jigawa State, the study area had a population estimated at 1,785,896 in the 2006 national census (NPC, 2006), and comprises eleven Local Government Areas (LGAs) falling within a 5 km buffer of the river: Auyo, Guri, Hadejia, Jahun, Kafin Hausa, Kaugama, Kiri Kasamma, Malam Madori, Miga, Ringim and Taura. The area encompasses two major dams and the Hadejia Valley Wetland. Flooding, exacerbated by climate change-induced shifts in rainfall patterns, is a recurrent disaster in the region, occurring annually during the rainy season and aggravated by inadequate drainage infrastructure and weak urban planning; addressing it through flood risk management strategies, including spatial planning and infrastructure development, is crucial for sustainable development (Babati et al., 2022).

The hydrology of the Hadejia River system is strongly influenced by the Tiga Dam (operational since 1974) on the Kano River and the Challawa Gorge Dam (operational since 1992) on the Challawa River (KNARDA, 2019). The river gains flow along the geological contact between the Basement Complex rocks and the Chad Formation (Kura et al., 2023). The Hadejia sub-basin, part of the Komadugu Yobe Basin, covers 43,970 km², with a long-term mean surface runoff of 72 $m^3\ s^{-1}$ (52 mm yr^{-1}; 2,274 MCM yr^{-1}), mean annual rainfall of 743 mm yr^{-1}, and an annual runoff coefficient of about 7% (KNARDA, 2019). Groundwater recharge for the Hadejia catchment has been estimated at 14, 13, 11, and 8 mm yr^{-1} for 2018, 2020, 2030, and 2040, respectively, corresponding to annual groundwater availability of 631, 575, 462, and 349 MCM yr^{-1} (KNARDA, 2019).

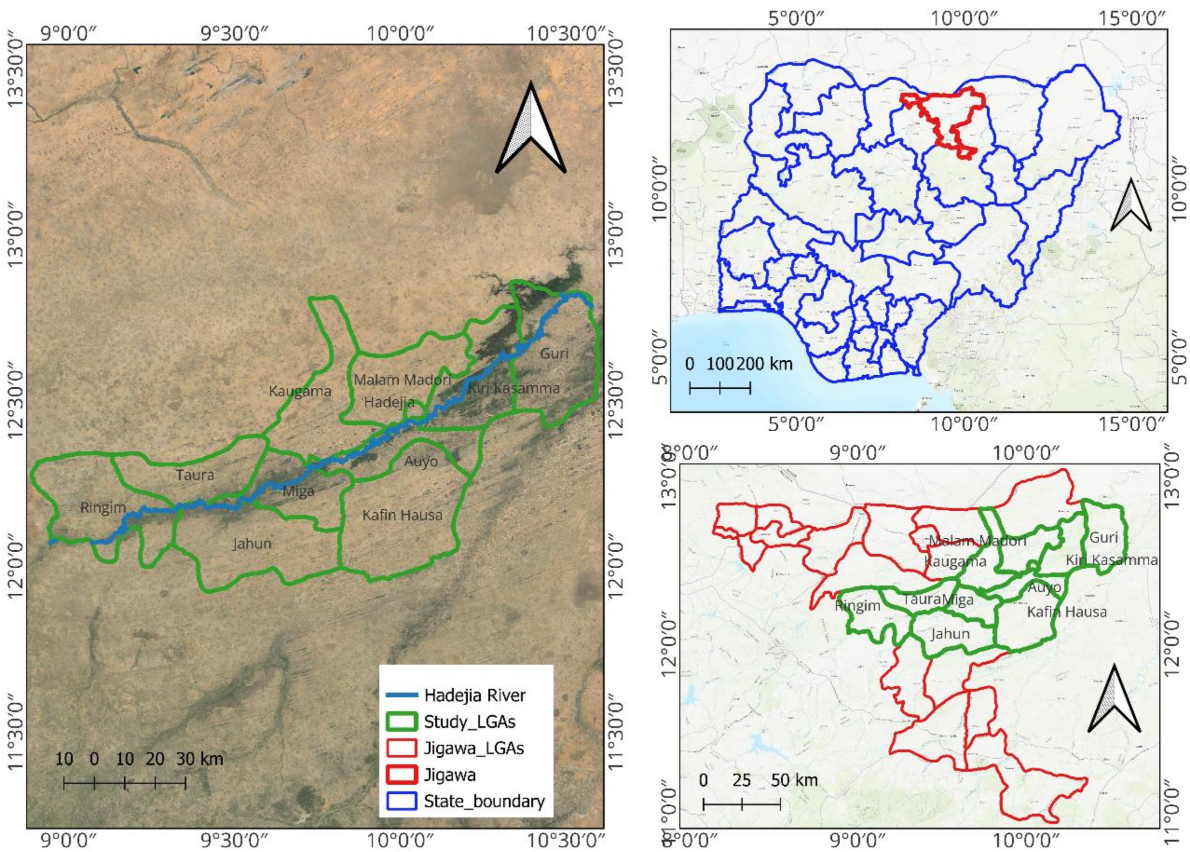

Figure 1: Location map of the study area

2.2 Data Collection

The datasets required for the study comprise both spatial and non-spatial attributes obtained from primary and secondary sources. Primary data consist of field observations and GPS coordinates collected during a three-phase field reconnaissance survey conducted between August 2023 and January 2024; these served as ground-truth data for training and validating the satellite image classification. Secondary data comprise medium-resolution satellite imagery – Sentinel-2A multispectral imagery (10 m spatial resolution) and the ALOS PALSAR Digital Elevation Model (DEM; 12.5 m resolution) – together with topographic and soil maps, administrative boundaries, hydrological records, historical rainfall and temperature data, and socioeconomic statistics (Table 1). The Sentinel-2A imagery was used for LULC mapping, while the DEM supported floodplain delineation and terrain modelling (slope, elevation, drainage density and topographic wetness). Gridded climatic data (CHIRPS rainfall and WorldClim temperature, 1981–2022) were used to characterise climate variability across the study LGAs. The integration of field-validated primary data with these secondary datasets enhanced the reliability of the spatial products used for flood risk assessment.

Table 1 summarises the datasets used, their sources and their purpose in the analysis.

Table 1: Datasets, sources and purpose

Type of Data	Source	Purpose
Rainfall data (1981–2022)	Climate Hazards Group InfraRed Precipitation with Station data (CHIRPS), accessed via Climate Engine	Climate variability and trend analysis
Sentinel-2A imagery (10 m)	United States Geological Survey (USGS) Earth Explorer	LULC mapping and NDVI derivation
ALOS PALSAR DEM (12.5 m)	Alaska Satellite Facility (ASF) Vertex	Elevation, slope, drainage density and TWI derivation
Administrative boundaries	Humanitarian Data Exchange (HDX)	Study area delineation and socioeconomic analysis
Soil map	FAO Harmonized World Soil Database v2.0	Soil texture and infiltration characterization
Flood inventory data	Questionnaire responses; NIHSA; SEMA; NEMA; HJRBDA records	Flood occurrence history and model validation
Soil moisture data	Copernicus Land Monitoring Service	Antecedent wetness characterization
Evapotranspiration data	NASA Earthdata (AppEEARS)	Water-balance and climatic characterization
Literacy rate data	National Bureau of Statistics (NBS), Nigeria	Socioeconomic vulnerability indicator
Road networks, rivers and water bodies	Satellite imagery; HDX	Distance-from-river and drainage analysis
Temperature data (1981–2022)	WorldClim v2.1	Climate variability and trend analysis

2.3 Flood Causative Factors

Sixteen flood causative factors were identified from a comprehensive review of flood susceptibility literature and from their documented relevance to Sudano-Sahelian environments (Table 2). The factors span three main criteria: meteorological (rainfall, temperature, evapotranspiration, NDVI), socioeconomic (LULC, literacy rate, population density), and hydrological (soil texture, slope, topographic wetness index, soil moisture, drainage density, distance from river, elevation, geology and lineament density). The number of factors was guided by three considerations: (i) completeness – the set must represent the hazard, the physical controls of runoff generation and concentration, and the socioeconomic conditions that shape exposure and vulnerability; empirical support each factor has been demonstrated to influence flood susceptibility in comparable semi-arid and data-scarce environments (Sani, 2008; Ali et al., 2020; Shuaibu et al., 2022; Mitra and Das, 2023; Almouctar et al., 2024); and data availability and independence only factors for which reliable spatial data exist at the basin scale, and that were not strongly redundant, were retained, the latter being verified through the multicollinearity screening described in Section 2.4. Together, the sixteen factors provide a comprehensive and regionally tailored basis for flood risk assessment.

Table 2: Flood causative factors used in the analysis

S/No	Main Criteria	Sub-criteria	Adapted from
1	Meteorological	Rainfall	Sani (2008); Ilyasu (2017)
2		Temperature	Sani (2008); Ilyasu (2017)
3		Evapotranspiration	Sani (2008); Ilyasu (2017)
4		Normalized Difference Vegetation Index (NDVI)	Kanani-Sadat et al. (2019); Ali et al. (2020); Mitra and Das (2023)
5	Socioeconomic	Land use/land cover	Sani (2008); Shuaibu et al. (2022)
6		Literacy rate	Shuaibu et al. (2022)
7		Population density	Shuaibu et al. (2022)
8	Hydrological	Soil texture	Mitra and Das (2023)
9		Slope	Sani (2008); Tudunwada & Abbas (2022)
10		Topographic Wetness Index	Tola and Shetty (2022)
11		Soil moisture	Talukdar et al. (2020)
12		Drainage density	Tudunwada and Abbas (2022)
13		Distance from river	Tudunwada and Abbas (2022)
14		Elevation	Shuaibu et al. (2022)
15		Geology	Mitra and Das (2023)
16		Lineament density	Periyasamy et al. (2020)

2.4 Data Processing and Analysis

Data processing followed a structured workflow comprising five stages: image acquisition and pre-processing; image classification and validation; terrain and thematic layer derivation; multicollinearity screening; and flood risk mapping using Multi-Criteria Decision Analysis (MCDA).

2.4.1 Image acquisition and pre-processing

Sentinel-2A scenes covering the study area were acquired for the 2013 and 2023 reference years. Atmospheric correction was performed with the Sen2Cor processor in the Sentinel Application Platform (SNAP), followed by radiometric calibration and resampling of all bands to 10 m. Pre-processed scenes were subsetted to the study extent and mosaicked in ENVI 5.3, and the Semi-Automatic Classification Plugin in QGIS was used to manage spectral signatures.

2.4.2 Image classification and accuracy assessment

LULC maps were produced using a supervised maximum-likelihood classification algorithm, with seven thematic classes: water body, dense vegetation, riparian vegetation, shrubland, farmland, built-up area and bare land. Training samples were digitised from high-resolution imagery and refined using the GPS ground-control points collected during the field surveys. Classification accuracy was evaluated with a standard error matrix using independent validation points; overall accuracy and the Kappa coefficient were computed, and only classifications achieving an overall accuracy of at least 85% were accepted for change detection. Final LULC maps and the 2013–2023 change trajectories were produced in ArcMap and ArcGIS Pro.

2.4.3 Terrain, climatic and thematic layer derivation

Elevation, slope, drainage density and the Topographic Wetness Index (TWI) were derived from the ALOS PALSAR DEM using standard hydrological tools in ArcGIS Pro; TWI was computed as $\ln(a/\tan\beta)$, where a is the specific catchment area and β is the local slope. Distance-from-river surfaces were generated by Euclidean distance from the digitised river network, and lineament density was mapped from lineaments extracted from hill-shaded DEM and satellite imagery. NDVI was computed from the Sentinel-2A near-infrared and red bands. Gridded CHIRPS rainfall and WorldClim temperature series (1981–2022) were summarised for each LGA, and the spatial distribution of annual mean rainfall across the flood-prone communities was interpolated using the Inverse Distance Weighting (IDW) method, which is appropriate for the modest station density of the study area.

2.4.4 Trend analysis

Temporal trends in annual rainfall and temperature were assessed with the non-parametric Mann–Kendall test, with the statistic reported as Kendall's τ, the significance level (p-value), and the Kendall score S. A five-year moving average was used to smooth inter-annual fluctuations and reveal decadal-scale tendencies. Flood occurrence records compiled from the questionnaire responses and institutional archives were analysed as a cumulative frequency series to characterise the long-run accumulation of reported flood events between 1984 and 2023.

2.4.5 Multicollinearity screening

Because many conditioning factors are spatially correlated, pairwise multicollinearity among the sixteen factors was examined using the Variance Inflation Factor (VIF) and tolerance statistics; factors with VIF $\geq$ 10 (tolerance $\leq$ 0.1) were considered redundant and were removed or combined before weighting.

2.4.6 Flood risk mapping using MCDA/AHP

The retained factors were integrated in a GIS environment using the Analytic Hierarchy Process (AHP), the most widely applied MCDA technique in flood susceptibility studies (Danumah et al., 2016; Radwan et al., 2019; Shuaibu et al., 2022; Aichi et al., 2024). A pairwise comparison matrix was constructed in which the relative importance of each factor was rated on Saaty's nine-point scale (Saaty, 1977), drawing on expert judgement informed by the field surveys and published evidence. Normalised weights were obtained from the principal eigenvector of the comparison matrix. The logical consistency of the judgements was verified with the Consistency Ratio (CR):

$$CR = CI / RI, \qquad \text{where } CI = (\lambda max - n) / (n - 1)$$

in which CI is the consistency index, λmax the principal eigenvalue of the matrix, n the number of factors, and RI the random consistency index for a matrix of order n. A CR below 0.10 was taken as indicating acceptable consistency; where CR exceeded this threshold, the pairwise judgements were revisited. Each factor layer was reclassified into a common ordinal susceptibility scale, multiplied by its AHP weight, and combined by weighted linear combination to produce the composite flood risk surface, which was then partitioned into susceptibility classes. The resulting risk map was validated against the independent flood inventory points, with predictive performance quantified using the Area Under the Receiver Operating Characteristic Curve (AUC), consistent with recent practice (Almouctar et al., 2024; Aichi et al., 2024).

3 Results

3.1 Climate Variability and Flood Risk

Figures 2 and 3 present the time series of annual rainfall and temperature for the Hadejia River Basin between 1981 and 2022, together with their corresponding five-year moving averages. These records are central to understanding how climate variability influences flood risk in the local government areas along the Hadejia River in Jigawa State.

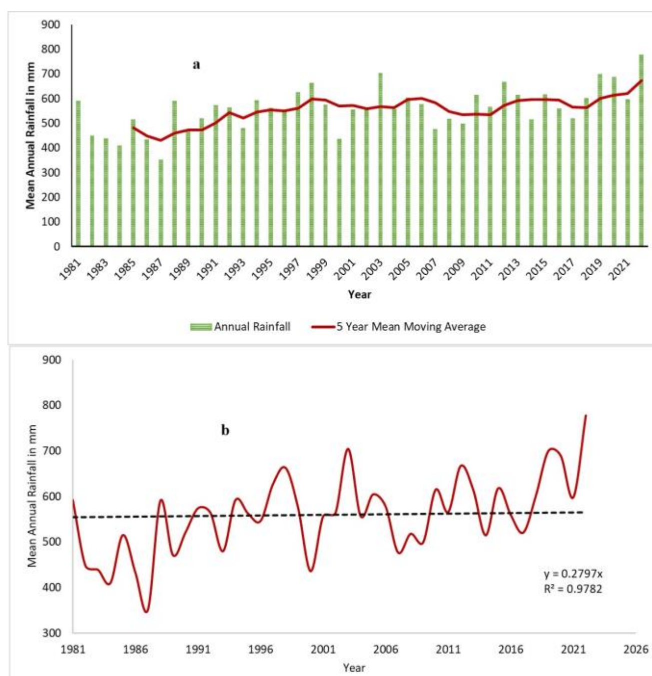

Figure 2: Annual rainfall in the Hadejia River Basin, 1981–2022: (a) annual totals with the five-year moving average; (b) time series relative to the long-term mean with fitted trend.

Rainfall exhibits pronounced inter-annual variability, with marked peaks in the late 1990s, early 2000s, and again from 2019 onwards (Figure 2). The year 2022 recorded the highest annual rainfall of the study period, 777.59 mm, with a five-year moving average of 673.06 mm, indicating a recent intensification of rainfall. Conversely, years such as 1984, 2000 and 2007 recorded substantially below-average totals. This variability is characteristic of the

Sudano-Sahelian zone, where rainfall is modulated by inter-annual and decadal-scale fluctuations in the West African monsoon and by remote ocean–atmosphere forcings (Nicholson, 2013; Biasutti, 2019). The five-year moving average reveals a quasi-systematic rise from the early 1990s, and the fitted trend line through the series confirms a positive long-term tendency. The recent increase is hydrologically significant: heavier and more concentrated rainfall raises surface runoff and river discharge, and the 2022 rainfall peak coincides with the severe flooding recorded across the basin in that year (Umar & Gray, 2023).

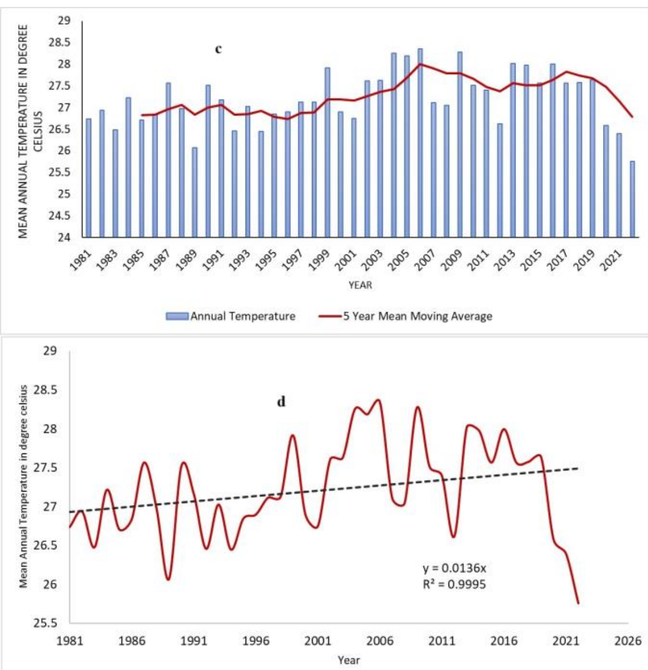

Figure 3: Annual mean temperature in the Hadejia River Basin, 1981–2022: (a) annual values with the five-year moving average; (b) time series with fitted trend.

Temperature shows a clearer long-term tendency (Figure 3). Annual mean temperatures fluctuated between 26.65 °C and 28.88 °C, with the highest value (27.92 °C on the smoothed series) recorded around 1999 and a sustained plateau of elevated temperatures thereafter; the five-year moving average reached its maximum of about 27.7 °C during 2016–2020. This gradual warming is consistent with regional and global patterns (Hirabayashi et al., 2013; IPCC, 2023). Rising temperatures intensify evapotranspiration and atmospheric moisture demand, altering the partitioning of rainfall between runoff and storage; in combination with the observed increase in rainfall, these favour both more intense flood events and more frequent moisture stress between events (Hirabayashi et al., 2013; IPCC, 2023).

Descriptive statistics and trend statistics for the two climatic variables are summarised in Table 3. Rainfall ranged from 390.70 mm to 874.41 mm, with a mean of 619.41 mm and a standard deviation of 95.33 mm, indicating moderate variability around the mean. The Mann–Kendall analysis returned a Kendall's τ of 0.377 (S = 294; p = 0.00049), indicating a statistically significant increasing trend in annual rainfall over 1981–2022: that is, later years in the series tend to record higher rainfall than earlier years. Temperature varied within a narrower band, 26.65–28.88 °C, with a mean of 27.87 °C and low dispersion (standard deviation = 0.56 °C); its Kendall's τ of 0.259 (S = 202; p = 0.019) likewise indicates a statistically significant, though weaker, warming trend. The temporal variable against which the trends were computed is the year of observation (1981–2022). These results demonstrate that the climate of the basin has become both warmer and wetter over the past four decades, with precipitation showing the stronger and more significant trend – a combination that directly elevates flood hazard.

Table 3: Descriptive statistics and Mann–Kendall trend analysis of climatic variables (1981–2022)

Statistic	Rainfall (mm)	Temperature (°C)
Minimum	390.70	26.65
Maximum	874.41	28.88
Mean	619.41	27.87
Standard deviation	95.33	0.56
Kendall's τ	0.377	0.259
p-value	0.00049	0.019
Kendall score (S)	294	202

The concurrence of a significant positive rainfall trend with significant warming mirrors projections by the Intergovernmental Panel on Climate Change of intensifying rainfall extremes over sub-Saharan Africa (IPCC, 2023) and is consistent with regional evidence that fluctuating but intensifying rainfall regimes aggravate flood risk in the basin (Nasidi et al., 2023; Umar & Gray, 2023). Compared with earlier analyses (e.g., Kheradmand et al., 2018), the present results reinforce the conclusion that climate change, expressed through rising temperatures and altered rainfall patterns, directly amplifies flood risk in vulnerable semi-arid basins. For the LGAs of Jigawa State, these trends imply that flood risk management must internalise climate variability – through enhanced flood forecasting, improved flood defences and climate-smart agriculture – while early-warning systems anchored on rainfall and temperature monitoring could further reduce impacts. Sustainable water management measures such as rainwater harvesting, improved irrigation scheduling and floodplain zoning would help communities manage the twin challenges of flood and drought (Wilby & Keenan, 2012; Nasidi et al., 2023; Umar & Gray, 2023).

3.2 Spatial Distribution of Rainfall across Flood-Prone Communities

Figure 4 compares the mean annual rainfall of the eleven flood-prone LGAs, computed by zonal statistics from the CHIRPS gridded dataset (1981–2022); the corresponding continuous rainfall surface (Figure 6a) was produced with the Inverse Distance Weighting interpolation described in Section 2.4. Mean annual rainfall is non-uniformly distributed, ranging from about 410 mm in Kiri Kasamma to about 869 mm in Miga. Miga (869.28 mm) and Ringim (868.97 mm) record the highest mean annual rainfall, followed by Hadejia (800.54 mm), Taura (794.37 mm) and Auyo (753.16 mm); the lowest totals occur in Kiri Kasamma (410.04 mm), Malam Madori (520.30 mm) and Kafin Hausa (531.23 mm). The spatial gradient broadly decreases from the south-west towards the north-east, consistent with the regional rainfall gradient of the Sudano-Sahelian zone (Nicholson, 2013). LGAs with higher mean totals – notably Miga, Ringim, Hadejia and Auyo, all of which straddle the river corridor – experience greater exposure to intense and prolonged precipitation, which increases surface runoff and flood risk; conversely, the drier north-eastern LGAs are comparatively less exposed to rainfall-driven flooding, although their proximity to the river keeps them within the floodplain hazard zone.

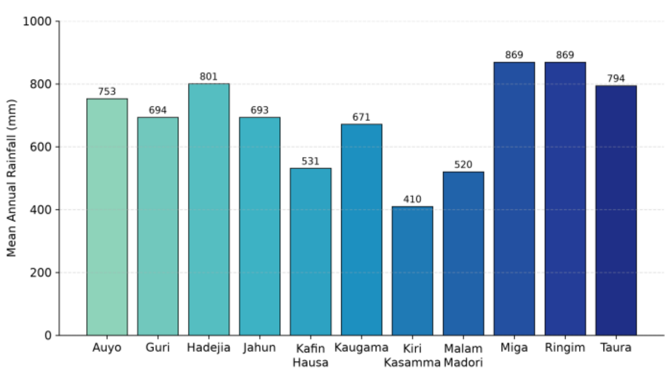

Figure 4: Mean annual rainfall of the eleven flood-prone LGAs of the study area (CHIRPS, 1981–2022).

3.3 Temporal Trend in Flood Occurrences

Figure 5 presents the frequency of recorded flood occurrences in the study area between 1984 and 2023, compiled from questionnaire responses and institutional flood inventories (NIHSA, SEMA, NEMA and HJRBDA). The fitted linear trend ($y = 10.69x - 21{,}249$; $R^2 = 0.776$) indicates that recorded occurrences increased on average by about 10.7 events per year over the study period; importantly, the regression coefficient expresses a change in the number of events per year, not an annual percentage change. The trend line accounts for a substantial share of the variance ($R^2 = 0.776$), underscoring the robustness of the upward tendency. During the 1980s and 1990s, occurrences remained comparatively low and fluctuated sharply (e.g., 1987, 1991, 1995 and 2000), reflecting episodic events rather than a sustained pattern. From the early 2000s onwards, the record shows a marked and more consistent rise, with fewer low-occurrence years, peaking at 538 recorded occurrences in 2022 – coinciding with the exceptional rainfall of that year – before declining to 336 in 2023, a drop that most plausibly reflects inter-annual variability in both flood events and reporting rather than a genuine reduction in hazard. This pattern suggests a transition from sporadic to more persistent and frequent flood conditions, although part of the apparent increase may also reflect improved event reporting and expanding exposure of population and assets in the floodplain (Umar & Gray, 2023).

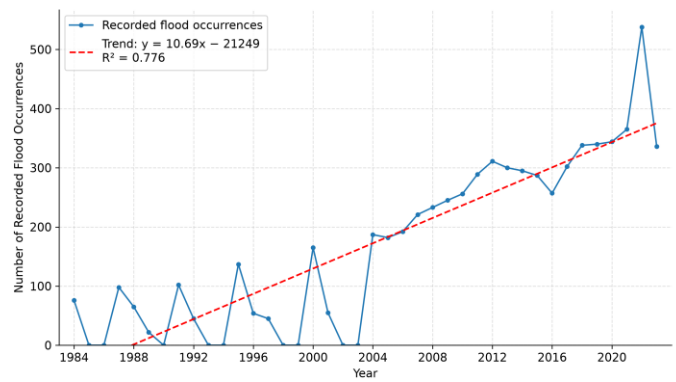

Figure 5: Time series of recorded flood occurrences in the study area, 1984–2023, with fitted linear trend.

The acceleration of flood occurrence since the early 2000s is consistent with the significant positive rainfall trend reported in Table 3 and with regional findings that reservoir regulation and land-use change along the Hadejia valley have modified the basin's flood regime (Shanono et al., 2023; Nasidi et al., 2023). It also aligns with the basin-wide modelling evidence of Babati et al. (2022), who projected rising flood magnitude and frequency in the Hadejia-Jama'are system. The coincidence of the record 2022 rainfall with the peak annual flood count strengthens the interpretation that hydro-climatic intensification is a primary proximate driver, superimposed on a progressively more exposed floodplain.

3.4 Spatial Characterisation of Flood Causative Factors

Figure 6 presents the spatial distribution of the sixteen flood causative factors across the study area, grouped into meteorological, socioeconomic and hydrological criteria. Among the meteorological factors, mean annual rainfall (Figure 6a) follows the south-west to north-east gradient described above, while mean annual temperature (Figure 6b) shows localised hot-spots around the central corridor.

Evapotranspiration (Figure 6c) and soil moisture (Figure 6d) jointly determine antecedent wetness: high evapotranspiration can temporarily deplete soil moisture, but this buffering is rapidly overwhelmed during the intense rainfall episodes that now characterise the wet season.

Among the socioeconomic factors, population density (Figure 6e) is highest along the river corridor and around the larger settlements, concentrating human exposure precisely where the hazard is greatest; literacy rates (Figure 6f) are spatially variable and condition the capacity of communities to interpret and act on early-warning information. The LULC map (Figure 6g) shows the dominance of farmland and shrubland, with built-up areas and farmland expanding along the river. Built-up areas and farmland expanded by 8 km² and 94 km² as quantified in Table 4, while water bodies and dense vegetation contracted by 10 km² and 6 km² (Table 4), reducing natural retention and interception and increasing runoff. Distance from the river (Figure 6h) exerts a first-order control: settlements cluster within the 1–3 km buffer, where inundation is most frequent.

The hydrological and terrain factors complete the risk picture. The low-relief terrain – elevation between 316 m and 422 m (Figure 6k) and slopes generally below 5° (Figure 6l) – impedes rapid drainage of the floodplain. High drainage density (Figure 6i) and high topographic wetness index values (Figure 6j) along the valley bottom indicate zones of flow convergence and prolonged saturation. Geologically, the aeolian sands and recent alluvium of the floodplain (Figure 6m) are highly permeable, but where they overlie the less permeable Chad Formation or Basement Complex, the subsurface storage capacity is limited, favouring saturation-excess runoff during sustained rainfall; lineaments (Figure 6n) locally enhance infiltration and groundwater exchange. NDVI (Figure 6o) shows that vegetation is densest along the riparian fringe and sparse over cultivated and bare areas, so that interception and infiltration are lowest exactly where human modification of the landscape is greatest. Soil texture (Figure 6p) – dominated by gleysols, fluvisols and regosols on the floodplain – is consistent with periodic waterlogging and limited infiltration once profiles are saturated.

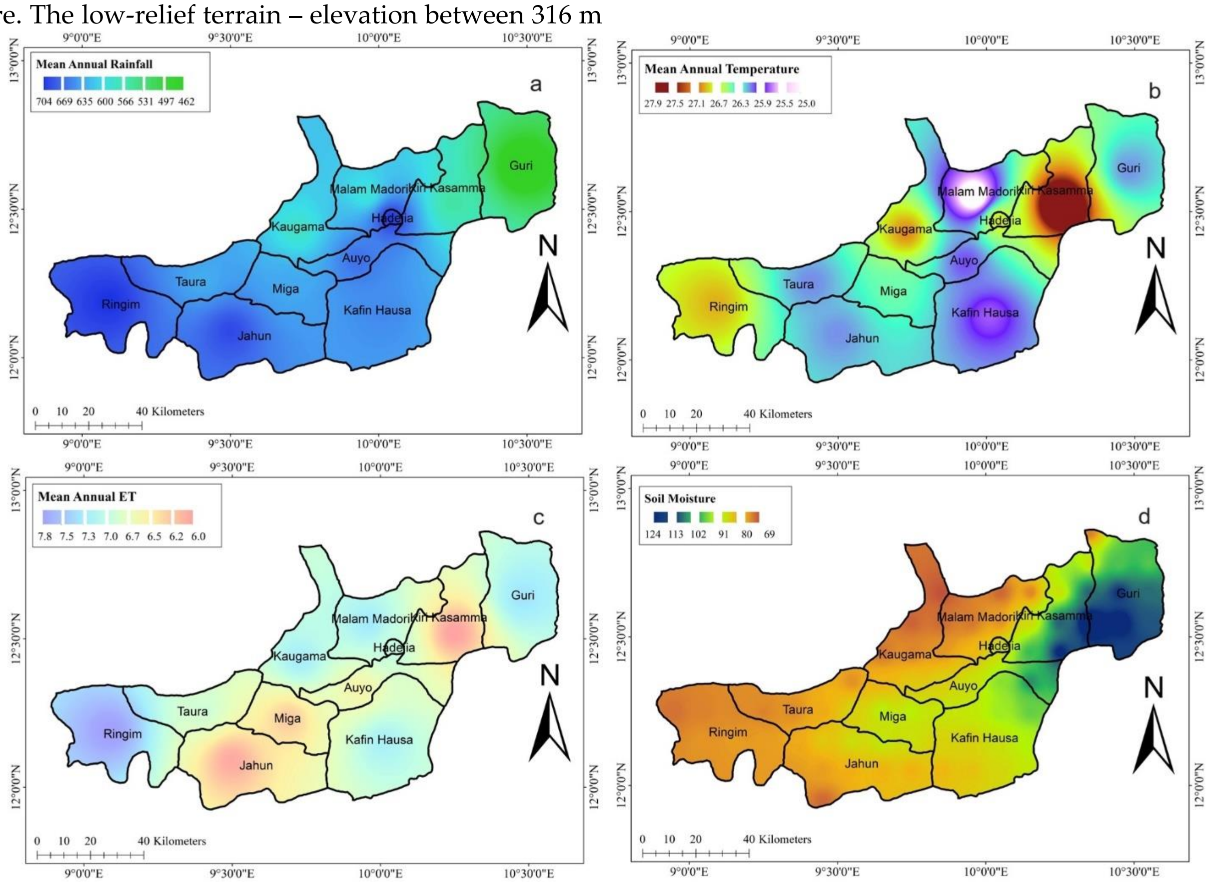

Figure 6 (panels a–d): Spatial distribution of flood causative factors – (a) mean annual rainfall; (b) mean annual temperature; (c) mean annual evapotranspiration; (d) soil moisture.

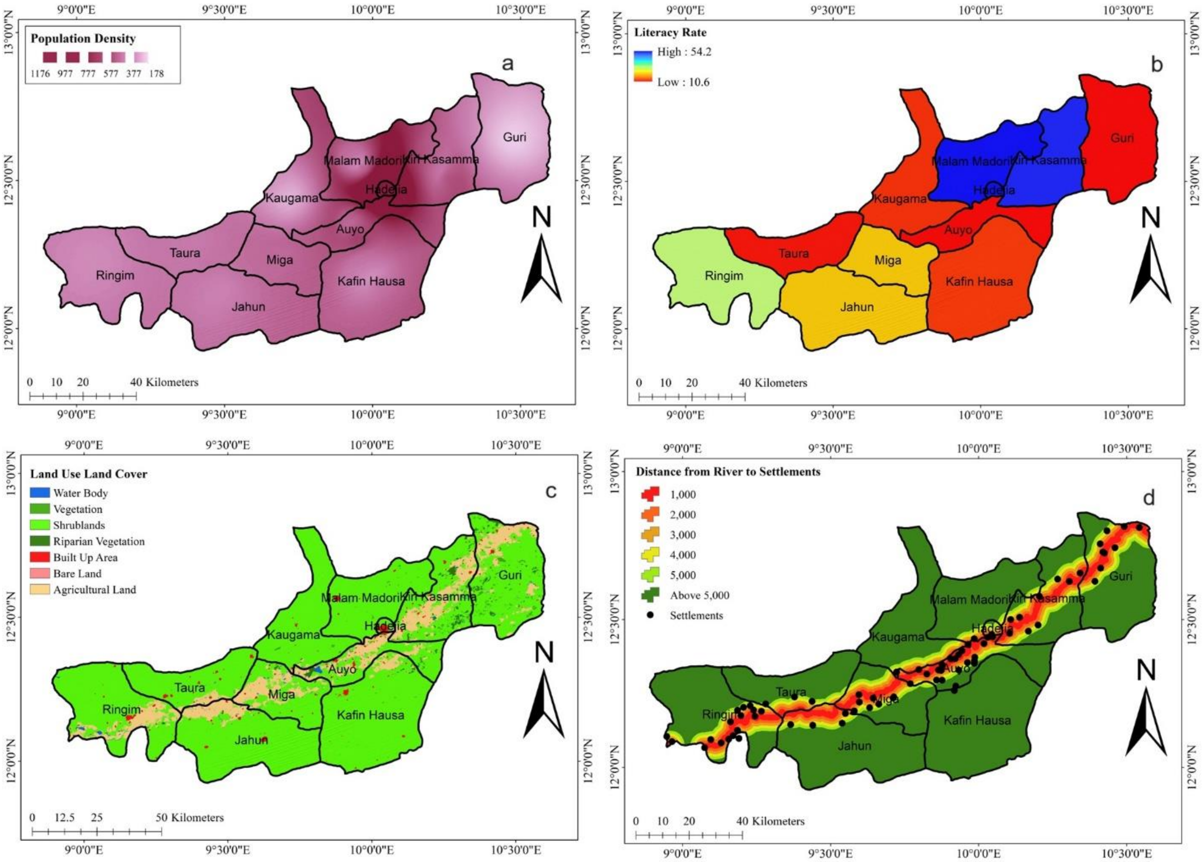

Figure 6 (panels e–h): (e) population density; (f) literacy rate; (g) land use/land cover; (h) distance from river to settlements.

Table 4: Land Use/Land Cover Change Statistics (2013 – 2023)

S/No	Class	Area km² (2013)	Percent	Area in Square km (2023)	Percent	Area Change	Percentage Cover Change	Annual Rate of Change (km2/year	Percentage of Annual Rate of Change (%/year)
1	Water Body	47.76	0.53	37.76	0.42	-10.00	-0.11	-1.00	-0.01
2	Dense Vegetation	48.43	0.54	42.43	0.47	-6.00	-0.07	-0.60	-0.01
3	Riparian Vegetation	98.00	1.09	97.00	1.08	-1.00	-0.01	-0.10	0.00
4	Farmland	1089.56	12.09	1183.56	13.13	94.00	1.04	9.40	0.10
5	Built-Up Area	89.90	1.00	97.90	1.09	8.00	0.09	0.80	0.01
6	Bare Land	0.75	0.01	0.91	0.01	0.17	0.00	0.02	0.00
7	Shrubland	7637.70	84.75	7552.53	83.80	-85.17	-0.95	-8.52	-0.09
	Total	9012.08	100.00	9012.08	100.00				

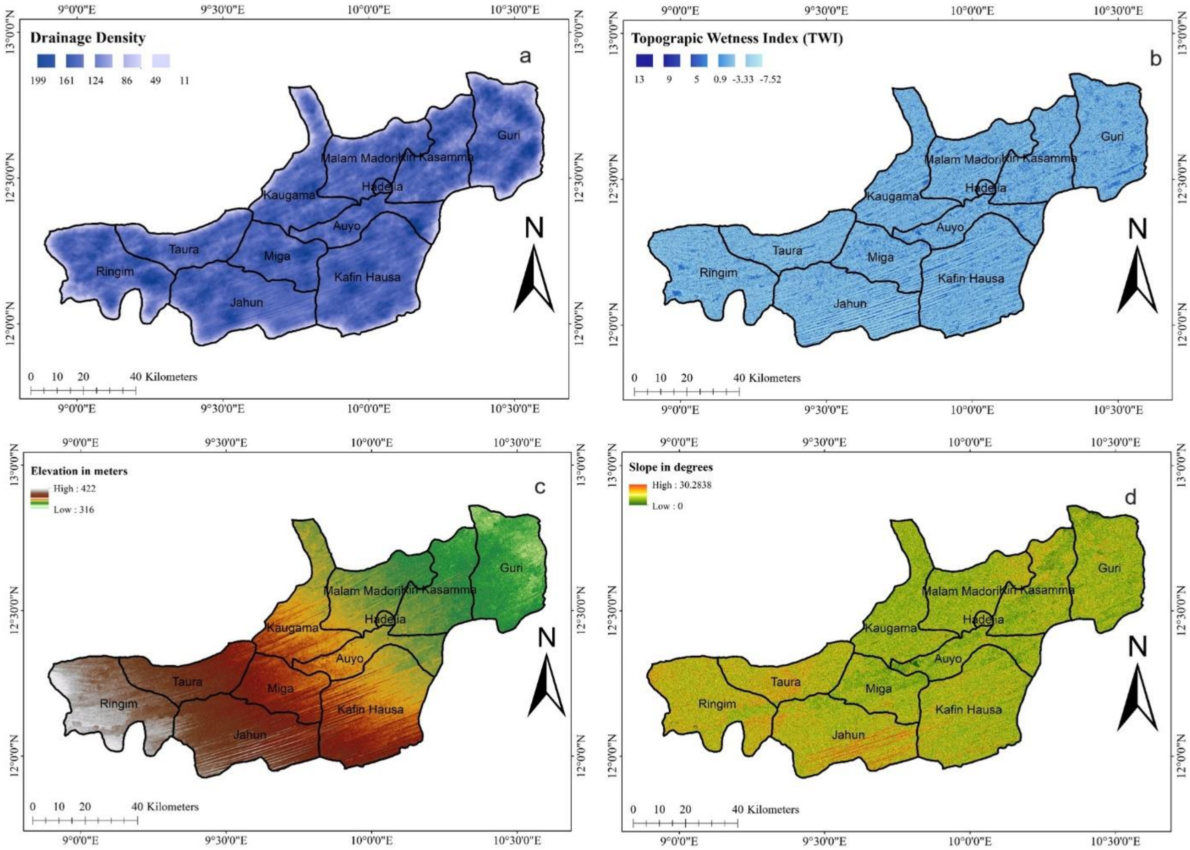

Figure 6 (panels i–l): (i) drainage density; (j) topographic wetness index; (k) elevation; (l) slope.

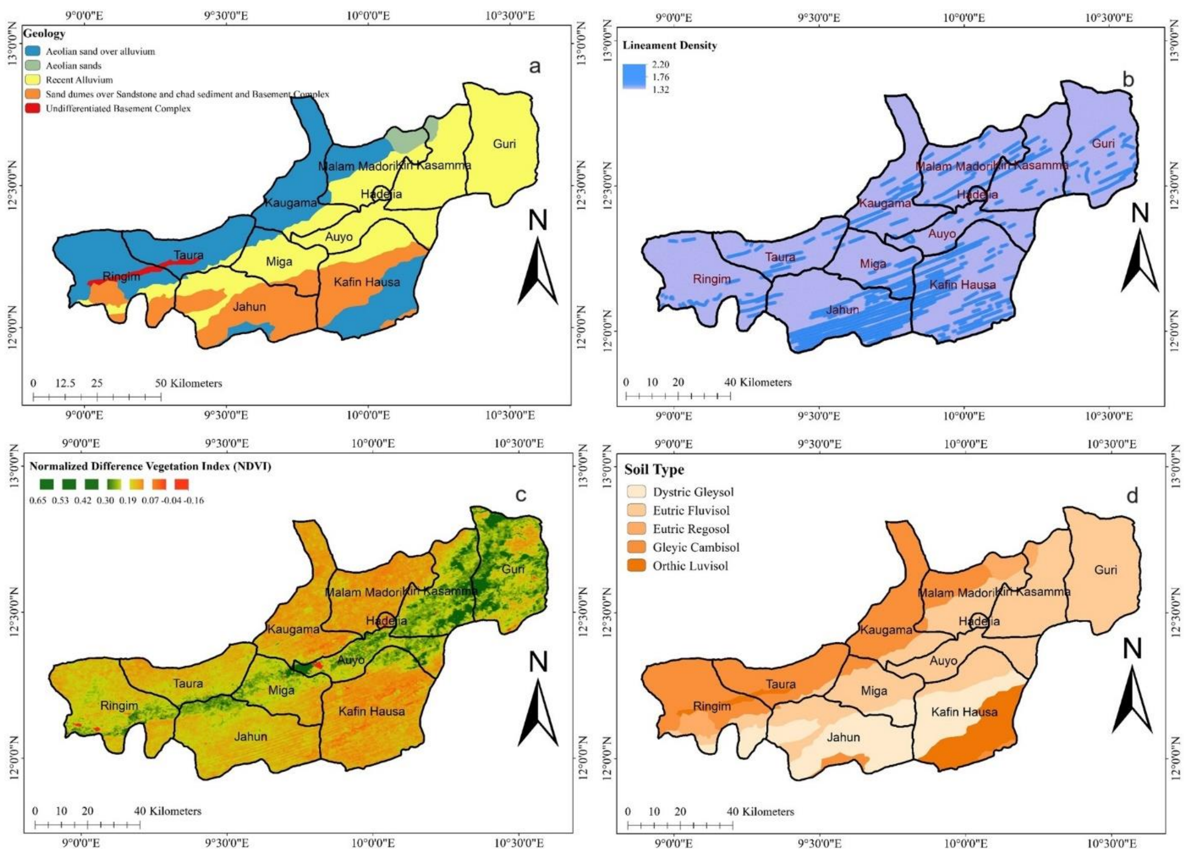

Figure 6 (panels m–p): (m) geology; (n) lineament density; (o) Normalized Difference Vegetation Index (NDVI); (p) soil type.

3.5 Flood Risk Assessment

The assessment of flood risk in the Hadejia River, using the Multi-Criteria Decision Evaluation (MCDE) and Analytic Hierarchy Process (AHP) techniques, reveals significant variations in risk levels across the region (Figure 7). The flood risk map statistics, as summarized in Table 5, categorize the area into five distinct risk levels: Very Low Risk, Low Risk, Moderate Risk, High Risk, and Very High Risk. Previous studies have demonstrated the effectiveness of these techniques in similar contexts. Jeb and Aggarwal (2008) applied remote sensing and GIS to model flood inundation hazards in the River Kaduna, revealing significant spatial variability in flood risk levels. Similarly, Yalcin and Akyurek (2004) used AHP for earthquake susceptibility mapping, which can be analogously applied to flood risk assessment.

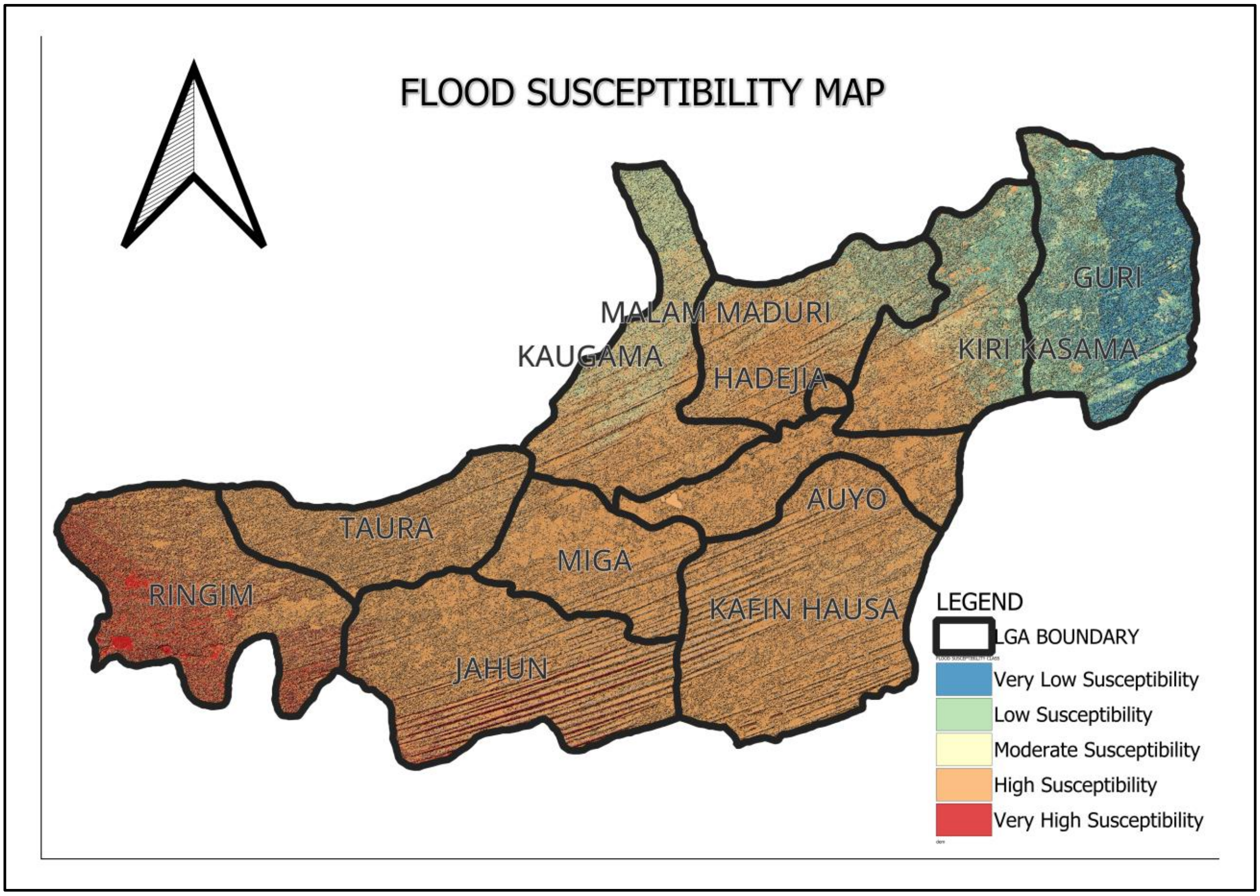

Figure 7: Flood Susceptibility Map

Table 5: Statistics of Flood Risk Map

S/No	Flood Risk Level	Area (Km²)	Percentage
1	Very Low Risk	3137.97	34.82
2	Low Risk	665.86	7.39
3	Moderate	1274.97	14.15
4	High Risk	3598.84	39.93
5	Very High Risk	334.38	3.71
Total		**9012.02**	**100.00**

The flood risk analysis of the Hadejia River Basin reveals significant spatial variability in flood susceptibility, categorized into five risk levels. The High-Risk category, encompassing 3598.84 km² (39,93%) of the area, represents nearly half of the total assessed region. This suggests that a substantial portion of the basin was impacted from effective natural and anthropogenic flood prevention measures, making these areas relatively unsafe from flooding. Similarly, the Very Low-Risk category, covering 3137.97 km² (34.82%), indicates regions that are generally safe. The effectiveness of measures is consistent with findings by Shuaibu et al. (2022), who emphasized the importance of GIS and multi-criteria decision analysis in managing environmental risks. Moderate Risk category includes 1274.97 km², accounting for 14.15% of the basin. This substantial portion of the area requires enhanced attention and planning to mitigate potential flood impacts. Meanwhile, the Very High-Risk areas, covering 334.38 km² (3.71%), are more prone to frequent and severe flooding. These regions demand significant intervention measures to protect both inhabitants and infrastructure, highlighting the need for robust flood control and emergency response systems. The low-risk category area at 665.86 km² (7.39%) represents the zones at low risk of flooding.

4 Discussion

Read together, the results reveal a coherent causal chain linking climate variability, land-use change and hydrological response in the Hadejia River Basin. The statistically significant intensification of rainfall (Table 3) increases the volume and peakedness of runoff delivered to a low-gradient river system whose floodplain has simultaneously been transformed: the 2013–2023 contraction of water bodies and dense vegetation and the expansion of farmland and built-up surfaces have reduced interception, depression storage and infiltration, so that a given storm now generates more rapid and larger runoff than it would have a decade earlier. This mechanism is consistent with experimental and modelling evidence from comparable African catchments, where conversion of vegetated land to cultivation and settlement has been shown to amplify flood peaks (Erena & Worku, 2018; Umar et al., 2019; Almouctar et al., 2024), and with findings from the Komadugu Yobe system that anthropogenic modification of the river valley, including reservoir operation, has altered flood timing and magnitude (Shanono et al., 2023). The socioeconomic layers indicate that exposure and vulnerability are spatially coincident with the hazard: the highest population densities and the lowest literacy rates occur in the same corridor communities – Hadejia, Auyo, Miga, Ringim – that combine the highest rainfall with immediate proximity to the river. The convergence of these three domains explains the post-2003 acceleration of recorded flood events better than any single driver, and it demonstrates the value of the integrated, multi-criteria approach adopted here relative to the single-theme analyses that dominate the earlier basin literature (Shuaibu et al., 2022; Tudunwada & Abbas, 2022; Kura et al., 2023).

These findings carry direct implications for flood risk management. The irregular inter-annual and inter-decadal variability of flood occurrences, and the absence of clear trends in maximum river discharge noted in earlier regional studies (Buma et al., 2016; Ibrahim et al., 2022), reinforce the need for predictive tools: hydrological models such as SWAT have proven effective for simulating streamflow and assessing flood risk under diverse climatic scenarios in the Hadejia-Nguru system (Ibrahim et al., 2022), and coupling such models with the susceptibility surfaces produced here would support scenario-based planning. At the community scale, the demonstrated role of vegetation loss and settlement encroachment argues for community-based flood management frameworks that combine structural measures (drainage improvement, flood defences, protected wetlands) with non-structural measures (land-use zoning, environmental education and livelihood diversification) (Nasidi et al., 2023; Wilby & Keenan, 2012). Finally, as Kundzewicz et al. (2018) emphasise, incorporating climate variability indices into flood risk assessment improves predictive skill and helps target adaptation; the integrated evidence presented here provides precisely the locally calibrated basis needed to operationalise that recommendation in one of Nigeria's most vulnerable basins.

5 Conclusion

This study set out to identify, quantify and spatially characterise the natural and anthropogenic factors driving flood risk in the Hadejia River Basin, Nigeria, by integrating field reconnaissance, satellite remote sensing, climatic trend analysis and GIS-based Multi-Criteria Decision Analysis. The main findings are fourfold. First, the climate of the basin has become significantly wetter and warmer over 1981–2022: annual rainfall shows a significant increasing trend (Kendall's $\tau = 0.377$, $p = 0.00049$) and temperature shows a weaker but significant warming trend ($\tau = 0.259$, $p = 0.019$), with the highest rainfall on record (777.59 mm) in 2022. Second, recorded flood occurrences have accumulated at an average rate of about eleven additional events per year since 1984, with a clear acceleration from the early 2000s and a peak annual count in 2022 that coincides with the exceptional rainfall of that year. Third, LULC change between 2013 and 2023, contraction of water bodies and dense vegetation, and expansion of farmland and built-up areas have reduced the basin's natural retention capacity and increased surface runoff. Fourth, the spatial analysis of sixteen causative factors shows that flood risk is concentrated in the river corridor communities (notably Hadejia, Auyo, Miga and Ringim), where high rainfall, immediate river proximity, low elevation, gentle slopes, high drainage density, sparse vegetation and dense population coincide.

The study contributes an integrated, spatially explicit evidence base that links climatic, hydrological and socioeconomic drivers of flood risk for one of Nigeria's most vulnerable basins, and its outputs have already informed the flood risk management activities of the Hadejia-Jama'are River Basin Development Authority and multi-stakeholder flood management forums. The findings imply that effective flood risk management in the basin must combine climate-informed early warning and forecasting, protection and restoration of wetlands and riparian vegetation, enforcement of floodplain zoning, and community-level adaptation supported by environmental education. The study is subject to limitations: the flood inventory relies partly on recall-based questionnaire data and institutional records whose completeness may have improved over time, which can exaggerate the apparent trend in occurrences; the AHP weights embody expert judgement and are therefore somewhat subjective; and the analysis is constrained by the resolution of the available DEM and gridded climate data. Future research should couple the susceptibility framework developed here with process-based hydrological modelling (e.g., SWAT) under climate change scenarios, extend the flood inventory with systematic gauge and remote-sensing-based event detection, and evaluate machine-learning alternatives to AHP for weighting and validating flood susceptibility models in data-scarce Sudano-Sahelian basins.

References

Abubakar, A., Sani, M., Ahmad, M. H., & Gambo, J. (2025). Geospatial flood risk mapping and vulnerability assessment using GIS and AHP in Hadejia River Basin, Jigawa State, Nigeria. FUDMA Journal of Sciences, 9(12). https://doi.org/10.33003/fjs-2025-0912-4323

Aderogba, K. A. (2012). Qualitative studies of recent floods and sustainable growth and development of cities and towns in Nigeria. International Journal of Academic Research in Economics and Management Sciences, 1(3), 1–25.

Aichi, A., Rais, J., Fikri, N., Kili, M., Kabbabe, B., & Hibti, M. (2024). Integrated GIS and analytic hierarchy process for flood risk assessment in the Dades Wadi watershed (Central High Atlas, Morocco). Results in Earth Sciences, 2, 100019. https://doi.org/10.1016/j.rines.2024.100019

Ali, S. A., Parvin, F., Pham, Q. B., Vojtek, M., Vojteková, J., Costache, R., Linh, N. T. T., Nguyen, H. Q., Ahmad, A., & Ghorbani, M. A. (2020). GIS-based comparative assessment of flood susceptibility mapping using hybrid multi-criteria decision-making approach, naïve Bayes tree, bivariate statistics and logistic regression: A case of Topľa basin, Slovakia. Ecological Indicators, 117, 106620. https://doi.org/10.1016/j.ecolind.2020.106620

Almouctar, M. A. S., Wu, Y., An, S., Yin, X., Qin, C., Zhao, F., & Qiu, L. (2024). Flood risk assessment in arid and semi-arid regions using multi-criteria approaches and remote sensing in a data-scarce region. Journal of Hydrology: Regional Studies, 54, 101862. https://doi.org/10.1016/j.ejrh.2024.101862

Babati, A. H., Abdussalam, A. F., Baba, S. U., & Isa, Z. (2022). Prediction of flood occurrences and magnitude in Hadejia-Jama'are River Basin, Nigeria. Sustainable Water Resources Management, 8(6), 188. https://doi.org/10.1007/s40899-022-00771-2

Biasutti, M. (2019). Rainfall trends in the African Sahel: Characteristics, processes, and causes. WIREs Climate Change, 10(4), e591. https://doi.org/10.1002/wcc.591

Buma, W. G., Lee, S. I., & Seo, J. Y. (2016). Hydrological evaluation of Lake Chad basin using spaceborne and hydrological model observations. Water, 8(5), 205. https://doi.org/10.3390/w8050205

Chukwuma, E. C., Okonkwo, C. C., Ojediran, J. O., Anizoba, D. C., Ubah, J. I., & Nwachukwu, C. P. (2021). A GIS-based flood vulnerability modelling of Anambra State using an integrated IVFRN-DEMATEL-ANP model. Heliyon, 7(9), e07868. https://doi.org/10.1016/j.heliyon.2021.e07868

Danumah, J. H., Odai, S. N., Saley, B. M., Szarzynski, J., Thiel, M., Kwaku, A., Kouame, F. K., & Akpa, L. Y. (2016). Flood risk assessment and mapping in Abidjan district using multi-criteria analysis (AHP) model and geoinformation techniques (Côte d'Ivoire). Geoenvironmental Disasters, 3, 10. https://doi.org/10.1186/s40677-016-0044-y

Eli, H. D., & Bariweni, P. A. (2020). Effects of seasonal characteristics of Kolo Creek flooding on farm-plot sizes in Central Niger Delta, Nigeria. Journal of Applied Sciences and Environmental Management, 24(5), 857–862.

Erena, S. H., & Worku, H. (2018). Flood risk analysis: Causes and landscape-based mitigation strategies in Dire Dawa city, Ethiopia. Geoenvironmental Disasters, 5, 8. https://doi.org/10.1186/s40677-018-0100-8

Hirabayashi, Y., Mahendran, R., Koirala, S., Konoshima, L., Yamazaki, D., Watanabe, S., Kim, H., & Kanae, S. (2013). Global flood risk under climate change. Nature Climate Change, 3(9), 816–821. https://doi.org/10.1038/nclimate1911

Ibrahim, U. A., Dan'azumi, S., Bdliya, H. H., Bunu, Z., & Chiroma, M. J. (2022). Comparison of WEAP and SWAT models for streamflow prediction in the Hadejia-Nguru Wetlands, Nigeria. Modeling Earth Systems and Environment, 8(4), 4997–5010. https://doi.org/10.1007/s40808-022-01379-3

Ibrahim, U. A., Yadima, S. G., & Nur Alkali, A. (2016). Flood frequency analysis at Hadejia River in Hadejia-Jama'are River Basin, Nigeria. Civil and Environmental Research, 8(9), 19–27.

Intergovernmental Panel on Climate Change (IPCC). (2023). Climate Change 2023: Synthesis Report. Contribution of Working Groups I, II and III to the Sixth Assessment Report of the Intergovernmental Panel on Climate Change. IPCC, Geneva, Switzerland. https://www.ipcc.ch/report/ar6/syr/

Kanani-Sadat, Y., Arabsheibani, R., Karimipour, F., & Nasseri, M. (2019). A new approach to flood susceptibility assessment in data-scarce and ungauged regions based on a GIS-based hybrid multi-criteria decision-making method. Journal of Hydrology, 572, 17–31. https://doi.org/10.1016/j.jhydrol.2019.02.034

Kheradmand, S., Seidou, O., Konte, D., & Batoure, M. B. B. (2018). Evaluation of adaptation options to flood risk in a probabilistic framework. Journal of Hydrology: Regional Studies, 19, 1–16. https://doi.org/10.1016/j.ejrh.2018.07.001

KNARDA. (2019). Water Audit for the Komadugu Yobe Basin: Main Report. Kano State Agricultural and Rural Development Authority / Komadugu Yobe Basin Strategic Action Programme, Kano, Nigeria.

Kundzewicz, Z. W., Hegger, D. L. T., Matczak, P., & Driessen, P. P. J. (2018). Flood-risk reduction: Structural measures and diverse strategies. Proceedings of the National Academy of Sciences, 115(49), 12321–12325. https://doi.org/10.1073/pnas.1818227115

Kura, N. U., Usman, S. U., & Khalil, M. S. (2023). Flood vulnerability assessment of a semi-arid region: A case study of Dutse in Jigawa State, Nigeria. Journal of Environmental Issues and Climate Change, 2(1), 20–29.

Mokhtari, E., Abdelkebir, B., Djenaoui, A., & Hamdani, N. E. H. (2024). Integrated analytic hierarchy process and fuzzy analytic hierarchy process for Sahel watershed flood susceptibility assessment, Algeria. Water Practice and Technology, 19(2), 453–475. https://doi.org/10.2166/wpt.2024.012

Nasidi, N. M., Shanono, N. J., Inuwa, A. Y., Zakari, M. D., Ibrahim, A., & Yahya, M. N. (2023). An appraisal of hydro-climatic impact on flash flood incidences at Hadejia River Valley watershed in Nigeria. FUDMA Journal of Sciences, 7(5), 134–140.

Nicholson, S. E. (2013). The West African Sahel: A review of recent studies on the rainfall regime and its interannual variability. ISRN Meteorology, 2013, 453521. https://doi.org/10.1155/2013/453521

NPC. (2006). Estimated Population Figures. National Population Commission of Nigeria, Abuja.

Ologunorisa, T. E., Obioma, O., & Eludoyin, A. O. (2022). Urban flood event and associated damage in the Benue Valley, Nigeria. Natural Hazards, 111(1), 261–282. https://doi.org/10.1007/s11069-021-05059-w

Periyasamy, S., Senthilkumar, P., Selvakumar, R., & Magesh, N. S. (2020). Delineation of groundwater potential zones using geospatial technique and analytical hierarchy process (AHP) in the hard rock terrain of southern India. Arabian Journal of Geosciences, 13, 1164.

Radwan, F., Alazba, A. A., & Mossad, A. (2019). Flood risk assessment and mapping using AHP in arid and semiarid regions. Acta Geophysica, 67, 215–229. https://doi.org/10.1007/s11600-018-0233-z

Saaty, T. L. (1977). A scaling method for priorities in hierarchical structures. Journal of Mathematical Psychology, 15(3), 234–281. https://doi.org/10.1016/0022-2496(77)90033-5

Sani, L. (2008). An assessment of flood vulnerability and adaptation levels in the Hadejia-Nguru wetlands, Nigeria. Journal of Applied Sciences Research, 4(11), 1512–1517.

Shanono, N. J., Attanda, M. L., Nasidi, N. M., Zakari, M. D., Ibrahim, A., Yahya, M. N., & Umar, S. I. (2023). Effect of reservoir utilization and other anthropogenic activities on the Hadejia River Valley floods: A review. FUDMA Journal of Sciences, 7(5), 125–133.

Shuaibu, A., Hounkpè, J., Bossa, Y. A., & Kalin, R. M. (2022). Flood risk assessment and mapping in the Hadejia River Basin, Nigeria, using a hydro-geomorphic approach and multi-criterion decision-making method. Water, 14(22), 3709. https://doi.org/10.3390/w14223709

Talukdar, S., Ghose, B., Shahfahad, Salam, R., Mahato, S., Pham, Q. B., Linh, N. T. T., Costache, R., & Avand, M. (2020). Flood susceptibility modeling in Teesta River basin, Bangladesh using novel ensembles of bagging algorithms. Stochastic Environmental Research and Risk Assessment, 34, 2277–2300. https://doi.org/10.1007/s00477-020-01862-5

Tola, A. D., & Shetty, A. (2022). Flood susceptibility assessment and prioritization using AHP and GIS in upper Awash sub-basin, Ethiopia. Environmental Challenges, 9, 100634. https://doi.org/10.1016/j.envc.2022.100634

Tudunwada, I. Y., & Abbas, A. (2022). Flood vulnerability mapping and prediction for early warning in Jigawa State, Northern Nigeria, using geospatial techniques. International Journal of Disaster Risk Reduction, 79, 103156. https://doi.org/10.1016/j.ijdrr.2022.103156

Umar, D. U. A., Ramli, M. F., Aris, A. Z., Jamil, N. R., & Tukur, A. I. (2019). Surface water resources management along Hadejia River Basin, northwestern Nigeria. Journal of Hydrology: Regional Studies (h2oj), 2(1), 184–199.

Umar, N., & Gray, A. (2023). Flooding in Nigeria: A review of its occurrence and impacts and approaches to modelling flood data. International Journal of Environmental Studies, 80(3), 540–561. https://doi.org/10.1080/00207233.2022.2081471

Wilby, R. L., & Keenan, R. (2012). Adapting to flood risk under climate change. Progress in Physical Geography, 36(3), 348–378. https://doi.org/10.1177/0309133312438908